JOURNAL OF AGRICULTURAL AND FOOD CHEMISTRY

Molecular Characterization of Compost at Increasing Stages of Maturity. 2. Thermochemolysis−GC-MS and ^{13}C-CPMAS-NMR Spectroscopy

RICCARDO SPACCINI* AND ALESSANDRO PICCOLO

Dipartimento Scienze del Suolo, della Pianta, e dell'Ambiente, Università di Napoli Federico II, Via Università 100, 80055 Portici, Italy

Off-line pyrolysis TMAH-GC-MS (thermochemolysis) and solid-state ^{13}C NMR spectroscopy were applied for the direct molecular characterization of composted organic biomasses after 60, 90, and 150 days of maturity. Off-line thermochemolysis of both fresh and mature composts released various lignin-derived molecules, the quantitative measurement of which was used to calculate structural indices related to compost maturity. These indicated that most of the molecular transformation occurred within the first 60 days of the composting process, whereas slighter molecular variations were observed thereafter. Both ^{13}C NMR spectra and offline pyrograms suggested that the process of compost maturity was characterized by a progressive decrease of alkyl components, whereas cellulose polysaccharides appeared to be more resistant and began to be transformed at a later composting period. The main components of the final mature compost were lignocellulosic material and hydrophobic alkyl moieties, inasmuch as that commonly found in well-humified organic matter of soils and sediments. The persistence of untransformed lignin-derived products and di- and triterpenoids throughout the maturity period suggested that these molecules are useful markers to both evaluate compost origin and trace its fate in the environment. Thermochemolysis provided the same characterization of molecules either unbound or bound to the compost matrix as that reached by a previously applied sequential chemical fractionation of the same compost materials, thereby indicating that thermochemolysis is a more rapid and equally efficient tool to assess compost molecular quality.

KEYWORDS: ^{13}C-CPMAS-NMR; offline pyrolysis; TMAH; compost maturity; plant biomarkers

INTRODUCTION

Recycling of organic biomasses in compost is important for both environmental quality and sustainable agriculture. Although application of composted organic matter to soil may increase soil physical quality and plant nutrition, it may also reduce mineralization of biolabile compounds, thereby enhancing the role of soil organic matter (SOM) as sink of organic carbon (*1*, *2*). Moreover, the content of humic matter in compost may be an important resource for soil remediation purposes (*3*, *4*).

In recent years, the transformation of organic components during composting was investigated to understand the extent of the inherent biological stabilization. This research was mainly aimed to characterize separates from compost such as dissolved organic matter (DOM) (*5*), humic-like components (*6*, *7*), extracted organic molecules (*8*), and lipid compounds (*9*). We concomitantly propose a chemical fractionation sequence to identify compost molecular components and differentiate the strength by which these are linked to the compost matrix (*10*). However, a direct molecular characterization of the bulk compost may also enlighten the process of organic matter stabilization by simultaneously determining all different organic molecules that are transformed during composting.

Both ^{13}C cross-polarization magic angle spinning nuclear magnetic resonance spectroscopy (^{13}C-CPMAS-NMR) and offline pyrolysis with tetramethylammonium hydroxide (TMAH) followed by gas chromatography−mass spectrometry (Pyr-TMAH-GC-MS) are updated and powerful tools for the molecular investigation of complex natural organic matter (*11*, *12*). The nondestructive solid-state ^{13}C NMR technique provides the distribution of organic carbons in a wide range of solid matrices and is currently applied to characterize the composition, as well as the transformation, of plant tissues, litter, SOM, and humic substances.

Pyrolysis in the presence of TMAH is increasingly used to study natural biopolymers such as plant waxes, cutins, and woods, as well as humic materials and bulk soil organic matter (*13*−*15*). It involves the solvolysis and methylation of ester and ether bonds present in the complex mixture of organic macromolecules and biopolymers, thereby enhancing both the thermal stability of acidic, alcoholic, and phenolic groups and their chromatographic detection. This technique consists more of a simultaneous thermochemolysis reaction rather than a pyrolysis

* Corresponding author (e-mail riccardo.spaccini@unina.it).

10.1021/jf0625407 CCC: $37.00
Published on Web 02/14/2007

followed by methylation of the polar compounds (*16*, *17*). Lower temperatures are then required for the concomitant solvolysis and methylation reactions, thereby reducing the secondary pyrolytic rearrangements. Moreover, the Pyr-TMAH-GC-MS technique conducted in the offline mode allows a more effective determination and quantitative measurement of pyrolytic products (*18*).

The main objective of this work was to characterize the molecular components of bulk compost samples at different degrees of maturity and to evaluate their transformation during the stabilization process of composting. The direct characterization of bulk compost samples was attempted by applying both solid-state ^{13}C NMR spectroscopy and offline Pyr-TMAH-GC-MS techniques, and the results were compared with those obtained by a previous stepwise chemical fractionation procedure (*10*).

MATERIALS AND METHODS

Compost Samples. The organic biomasses used in compost production (GeSeNu SrL, Perugia, Italy) had the following composition: 50% domestic organic wastes, 40% refuse from plant trimming, and 10% vegetal residues from tobacco and aromatic plants. These materials were mixed, ground, and sieved at 12 mm. Compost products were obtained aerobically after 30 days of a common active phase, followed by three curing phases of an additional 30, 60, or 120 days, which yielded, respectively, compost samples 60, 90, and 150, of different maturities. Before analysis, compost samples were oven-dried at 40 °C until constant weight and sieved at 500 μm.

Solid-State ^{13}C NMR Spectroscopy. Solid-state NMR spectroscopy (^{13}C-CPMAS-NMR) was performed on a Bruker AV-300 equipped with a 4 mm wide-bore MAS probe. NMR spectra were obtained by applying the following parameters: 13000 Hz of rotor spin rate; 1 s of recycle time; 1 ms of contact time; 20 ms of acquisition time; 5000 scans. Samples were packed in 4 mm zirconia rotors with Kel-F caps. The pulse sequence was applied with a ^{1}H ramp to account for nonhomogeneity of the Hartmann−Hahn condition at high spin rotor rates. Given the large bandwidth and the lower resolution of the ^{13}C-CPMAS-NMR spectroscopy, the overall chemical shift range is usually divided in the following main resonance regions: alkyl-C (0−60 ppm); O-alkyl-C (60−110); aromatic and aromatic substituted C (110−160 ppm); carboxyl and carbonyl C (160−200 ppm).

Offline Pyrolysis TMAH-GC-MS. About 100 mg of dried compost was placed in a quartz boat and moistened with 1 mL of TMAH (25% in methanol) solution. After drying the mixture under a gentle stream of nitrogen for about 10 min, the sample was introduced into a Pyrex tubular reactor (50 cm × 3.5 cm i.d.) and heated at 400 °C for 30 min (Barnstead Thermolyne 21100 furnace). The released products of thermochemolysis were continuously transferred by a helium flow (100 mL min^{-1}) into two successive chloroform (50 mL) traps kept in ice/salt baths. The chloroform solutions were combined in a round flask and concentrated by rotoevaporation. The residue was redissolved in 1 mL of chloroform and transferred in a glass vial for GC-MS analysis. Three replicates of thermochemolysis were carried out for each compost sample.

The GC-MS analyses were conducted with a Perkin-Elmer Autosystem XL equipped with an RTX-5MS WCOT capillary column (Restek, 30 m × 0.25 mm; film thickness = 0.25 μm) and coupled, through a heated transfer line (300 °C), with a PE Turbomass-Gold quadrupole mass spectrometer. Chromatographic separation was achieved with the following temperature program: 60 °C (1 min isothermal), raised at 7 °C min^{-1} to 100 °C and then at 4 °C min^{-1} to 320 °C (10 min isothermal). Helium was the carrier gas at 1.90 mL/min, the injector temperature was at 250 °C, and the split injection mode had a 30 mL/min of split flow. Mass spectra were obtained in EI mode (70 eV), scanning in the range of *m*/*z* 45−650, with a cycle time of 1 s. Compound identification was based on comparison of mass spectra with the NIST library database, published spectra, and real standards.

For quantitative analysis, due to the large variety of detected compounds with different chromatographic responses, external calibration curves were built by mixing methyl esters and/or methyl ethers of the following molecular standards: tridecanoic acid, octadecanol, 16-hydroxyhexadecanoic acid, docosandioic acid, β-sitosterol, and cinnamic acid. Increasing amounts of standard mixtures were placed in a quartz boat and moistened with 0.5 mL of TMAH (25% in methanol) solution. The same thermochemolysis conditions as for compost samples were applied for the standards. The percentage recovery of standards ranged from 82 to 91% of initial amount.

Labile Carbohydrates. To evaluate the biolability of carbohydrate compounds, alkyl compounds were first removed from compost samples by the sequential procedure outlined earlier (*10*), which consisted of (1) extraction in an organic solvent, (2) BF_3−MeOH transesterification, and (3) KOH−MeOH solvolysis. Easily hydrolyzable carbohydrates were removed from this simplified compost matrix by an overnight extraction with dilute sulfuric acid (0.5 M, 1/10 w/v) (*19*). The resulting solid residue was extensively washed with deionized water until neutral pH and freeze-dried before being subjected to ^{13}C-CPMAS-NMR spectroscopy.

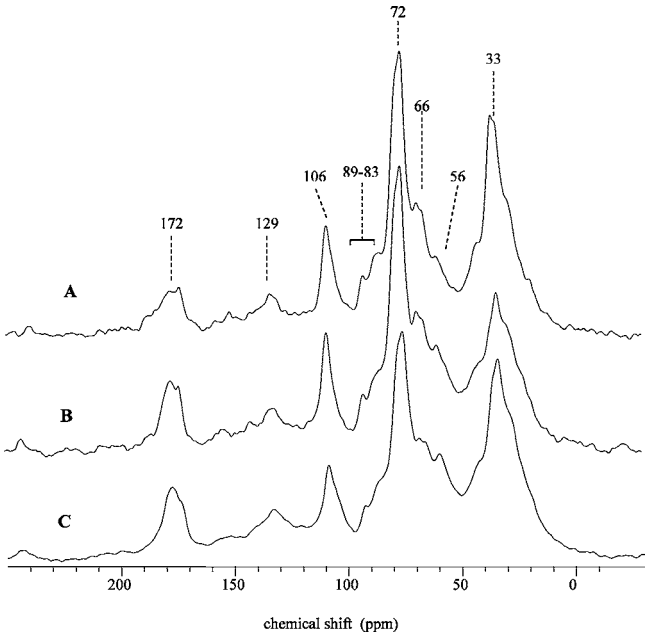

Figure 1. ^{13}C-CPMAS-NMR spectra of bulk compost samples at increasing maturity stages: (**A**) compost 60; (**B**) compost 90; (**C**) compost 150.

Table 1. Relative Distribution (Percent) of Signal Area over Chemical Shift Regions (Parts per Million) in ^{13}C-CPMAS-NMR Spectra of Compost Samples

sample	0–60	60–110	110–160	160–200	HB/HI[a]
compost 60	37.6	50.8	7.2	4.3	0.81
compost 90	30.6	56.1	7.3	6.1	0.61
compost 150	45.3	37.6	9.6	7.4	1.22

[a] Hydrophobic carbons/hydrophilic carbons = [(0 − 60) + (110 − 160)/(60 − 110) + (160 − 200)].

RESULTS AND DISCUSSION

NMR Spectra. The ^{13}C-CPMAS-NMR spectra of bulk compost samples at increasing stage of maturities are shown in **Figure 1**, whereas the relative distribution of signal areas is reported in **Table 1**. The spectrum of the less mature compost 60 was dominated by the signal in the alkyl-C (0−60 ppm) and O-alkyl-C (60−110 ppm) regions. The former region is composed by carbons in $(CH_2)_n$ and terminal CH_3 groups of plants lipid compounds, such as waxes and aliphatic biopolyesters. Plant woody tissues were also indicated by the 56

ppm shoulder of methoxy groups on aromatic rings of guaiacyl and siringyl units of lignin structures (*20*). The resonances in the O-alkyl-C region are assigned to monomeric units in oligo- and polysaccharidic chains of plant woody tissues (*21*). The intense signal around 72 ppm corresponds to the overlapping resonances of C2, C3, and C5 carbons in the pyranoside structure of cellulose and hemicellulose, whereas the signals at 106 ppm (sharp), 65 ppm, and 82−85 ppm (shoulders) are assigned to the anomeric C1 carbon and the C6 and C4 carbons, respectively, the latter being split in the presence of both amorphous and crystalline forms of cellulose (*22*). The aromatic region (110−160 ppm) did not reveal the distinct resonances of ring carbons in lignin structures (*23*). Only a weak broad band around 130 ppm may be related to *p*-hydroxyphenyl rings of cinnamic units in both lignin and suberin biopolymers. A prominent signal for quaternary carbons at 172 ppm is currently assigned to carboxyl groups.

A decrease of alkyl carbons was shown for the sample after 90 days of composting (**Figure 1B** and **Table 1**), suggesting an overall mineralization of the most bioavailable lipid compounds. No equivalent changes were revealed for carbohydrate carbons, except for the significant reduction of the 83 ppm shoulder assigned to noncrystalline cellulose. Conversely, a relatively larger decrease of the carbohydrate region was shown for compost at the final stage of maturity (**Figure 1C** and **Table 1**). In this sample, the significant residual carbohydrate and alkyl carbons, as well as the increased content of methoxyl and aromatic carbons, suggested a predominance of lignocellulosic and recalcitrant hydrophobic materials. The increased hydrophobicity of compost 150 with respect to less mature samples is shown by the hydrophobic C/hydrophilic C ratio (HB/HI) in **Table 1**.

To evaluate whether the carbohydrate carbons belonged to labile mono- or recalcitrant polysaccharides, the compost materials were subjected to a mild stepwise purification procedure (*10*) and removal of labile carbohydrates, which should have left unaltered the glycosidic bonds of polysaccharides. The 60−110 ppm region of NMR spectra of all compost residues after such purification (**Figure 2A−C**) closely resembled that of cellulose from plant woody tissues (*21, 24*), suggesting that a large part of carbohydrates consisted of polysaccharide components of plant cellulose fibers. This indicated a biological stability of cellulose content in the less stable compost and only an incipient decomposition during the last period of the compost curing phase. Conversely, the lack of changes for both aromatic and methoxyl lignin components was confirmed also in these purified compost samples.

Offline Pyr-TMAH-GC-MS. The total ion chromatograms (TIC) derived from the thermochemolysis of less mature compost 60 and mature compost 150 are shown in **Figure 3**. The compounds identified in the compost samples are listed in **Table 2**, whereas their quantitative evaluation is shown in **Table 3**. Thermochemolysis of the bulk composts released more than 100 different molecules, which were identified as methyl ethers and esters of natural compounds (**Table 2**). The majority of these compounds originated from higher plants and were represented by lignin, waxes, and aliphatic biopolymers. These findings on compost samples are similar to other results on bio- and geochemical materials (*25, 26*) and validate the effectiveness of the offline Pyr-TMAH-GC-MS technique in the investigation of complex organic materials.

Contrary to the indications of ^{13}C NMR spectra, low amounts of carbohydrates were found among the pyrolysis products. Only a few peaks reconducible to polysaccharides, such as trimethoxy

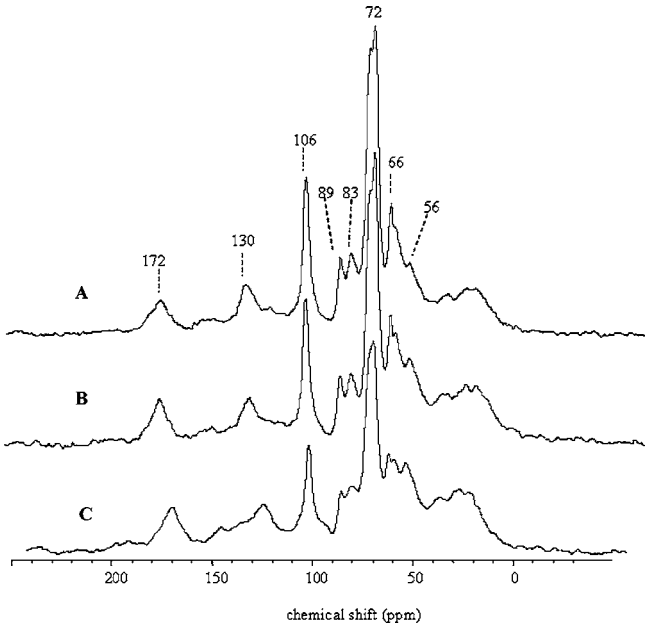

Figure 2. ^{13}C-CPMAS-NMR spectra of solid residues from compost samples after removal of alkyl components and acid hydrolysis of low molecular weight carbohydrates: (**A**) compost 60; (**B**) compost 90; (**C**) compost 150.

benzene isomers and methyl ether derivatives of monosaccharides, were found in the various chromatograms (**Table 2**). A pyrolysis product, which was possibly assigned to an oligosaccharide, was found only in the pyrogram of compost 150 (**Figure 3B**). The lack of polysaccharidic compounds was already noted in applications of thermochemolysis on plant woody tissues and soil organic matter (*13, 27*). It was pointed out that although conventional flash pyrolysis may produce carbohydrate derivatives, the offline TMAH pyrolysis appears to be less prone to the detection of polysaccharides in complex geochemical matrices. Works on model compounds showed that parameters such as TMAH content and temperature and time of pyrolysis should be carefully set up for different substrates if carbohydrate products are to be made visible in pyrograms (*28*). In the present work, the evaluation of OC content in compost samples before and after pyrolysis revealed that about 50% of the initial OC remained in the solid residue. It is thus conceivable that, also for compost samples, the current setup of thermochemolysis parameters is highly selective for lignin and alkyl components and reduces the simultaneous identification of carbohydrate units from cellulose.

Lignin Compounds. The number of lignin components released by thermochemolysis of compost 60 (**Figure 3A**) closely resembles that obtained for lignocellulose fractions of plant tissues and plant debris (*21, 29*). The different lignin derivatives (**Tables 2** and **3**) are associated with current symbolism in thermochemolysis analysis for lignin basic structures: P, *p*-hydroxyphenyl; G, guaiacyl (3-methoxy, 4-hydroxyphenyl); and S, syringyl (3,5-dimethoxy, 4-hydroxyphenyl) (*23, 30*).

The amount of various methylated *p*-hydroxyphenyl, guaiacyl, and syringyl derivatives released from compost confirms the origin of lignin from different higher plants. The softwood of gymnosperms is made up almost exclusively of guaiacyl subunits, whereas both syringyl and guaiacyl units constitute the hardwood of perennial angiosperm, and all three components are building blocks of grass lignin, the *p*-hydroxyphenyl unit being the major constituent (*31*).

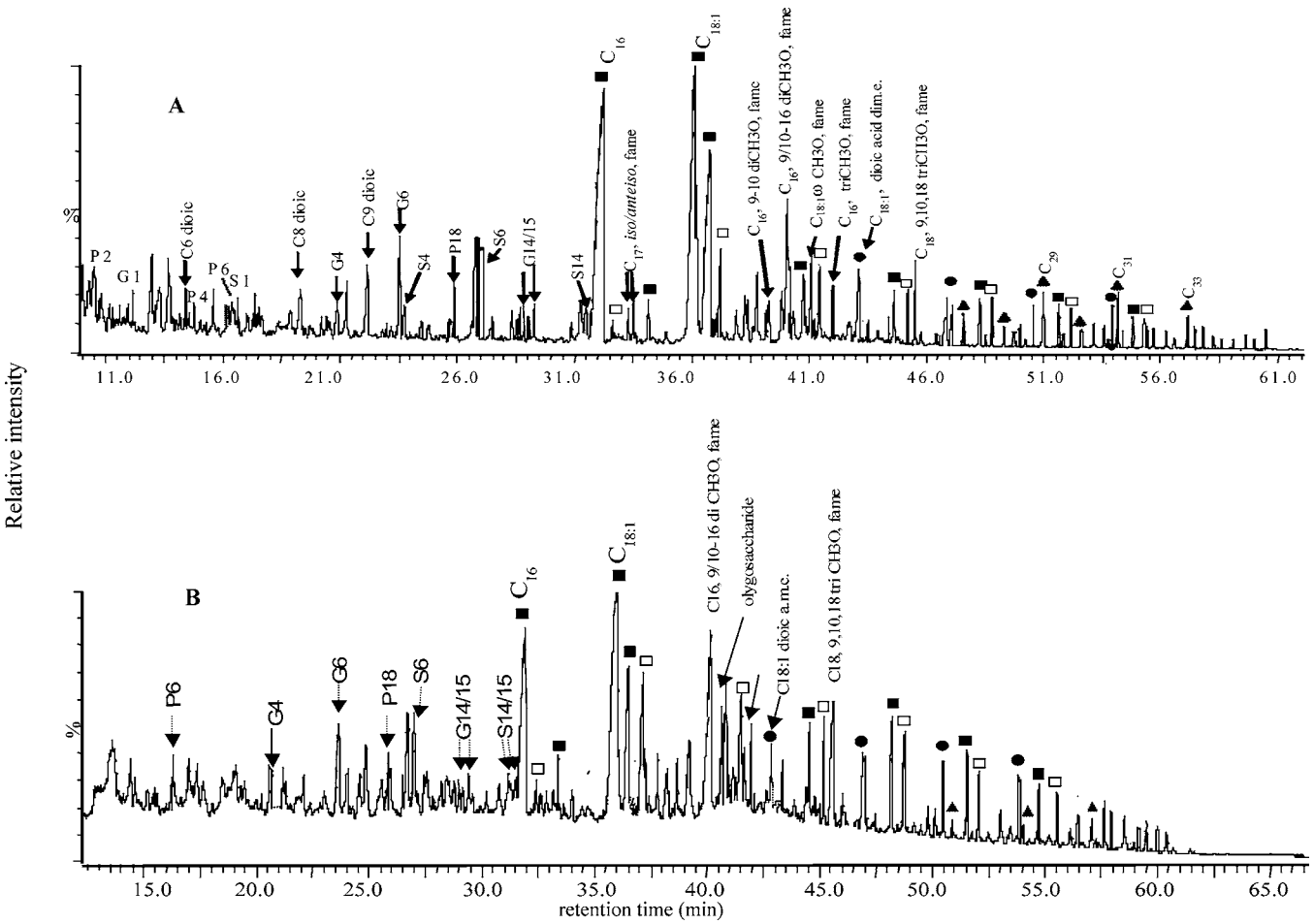

Figure 3. Total ion chromatograms of thermochemolysis products: (**A**) compost 60; (**B**) compost 150; (■) FAME; (□) ω-hydroxy-FAME; (●) alkanedioic acid DIME; (▲) *n*-alkanes.

The main lignin components released from compost 60 were the respective oxidized products of both di- and trimethoxy phenylpropane molecules, such as benzaldehyde (G4, S4), acetophenone (G5, S5), and benzoic acid (G6, S6) units (**Table 2**). Other important and classical products of lignin thermochemolysis were the cis and trans isomers of 1-(3,4-dimethoxyphenyl)-2-methoxyethylene (G7, G8) and 1-(3,4,5-trimethoxyphenyl)-2-methoxyethylene (S7, S8), as well as the enantiomers of 1-(3,4-dimethoxyphenyl)-1,2,3-trimethoxypropane (G14 and G15), and 1-(3,4,5-trimethoxyphenyl)-1,2,3-trimethoxypropane (S14 and S15). 3-(4-Methoxyphenyl)-2-propenoic acid (P18) was the most abundant P product, which may have resulted from both the oxidation of *p*-hydroxyphenyl units in lignin and the aromatic domains of suberin biopolymers in plant woody tissues. Compost maturity did not imply a significant variation in the total amount of guaiacyl and syringyl lignin components. Conversely, a decrease was noted for the *p*-hydroxyphenyl units (**Table 3**), which were represented only by the P6 and P18 components in the final compost 150. This behavior may be explained by the less complex structure of grass lignin, which leaves the phenylpropanoid units more exposed to bio-oxidation.

All of these released products may be used as plant biomarkers to trace the biodegradation of plant straw and woody tissues and evaluate the fate of organic matter in soils (*30*, *32*). The extent of lignin degradation may thus be estimated by structural indices that are based on the relative amount of specific guaiacyl and syringyl thermochemolysis products (*23*). These include the G4,S4 and G6,S6 derivatives, as well as the threo/erythro isomers of 1-(3,4-dimethoxyphenyl)-1,2,3-trimethoxypropane (G14 and G15) and 1-(3,4,5-trimethoxyphenyl)-1,2,3-trimethoxypropane (S14 and S15) (**Table 2**). Whereas the aldehydic and acidic forms of guaiacyl and syringyl structures result from progressive lignin oxidation, the corresponding homologues with a methoxylated side chain are indicative of unaltered lignin components, which retain the propyl ether intermolecular linkages. Therefore, Ad/Al and Γ indices are, respectively, the ratio of peak areas of acidic structures over that of the corresponding aldehydes (G6/G4, S6/S4) and over the sum of peak areas for the threo/erythro isomers (Γ_G = G6/[G14 + G15]; Γ_S = S6/[S14 + S15]). These indices are considered to be good indicators of the bio-oxidative transformation of lignin polymers (*21*).

In this work, the chromatographic coelution of S15 with the front of the large hexadecanoic acid methyl ester peak (**Figure 3A**) undermined the correct evaluation of the S15 peak area, thereby hindering the full estimation of the Γ_S parameter. Moreover, the use of mass base peaks for methyl palmitate (*m*/*z* 74) and S15 (*m*/*z* 211) to evaluate their different contributions, as suggested elsewhere (*30*), was not helpful due to the predominance of the fatty acid methyl ester and consequent masking of the S15 peak. Nevertheless, both Ad/Al and Γ_G ratios for the less mature compost 60 (**Table 3**), as compared to analogous data reported in the literature for both fresh and decomposed woody tissues (*30*, *33*), suggest an advanced lignin decomposition during the first composting period. Conversely, no significant changes were revealed by these structural indices

Table 2. Thermochemolysis Products[a] Released from Compost Samples

RT[b]	compound	type	RT	compound	type
10.3	benzene, 4-OMe, 1-methyl	Lg P2	38.4	10-OMe C_{18} FAME	Bp
11.3	benzene, 4-OMe, 1-ethenyl	Lg P3	38.8	pimaric acid ME	Dt
11.6	3,4-di-OMe benzene	Lg G1	39.3	9,10-diOMe C_{16} FAME	Bp
12.9	*n*-C_8 FAME	Lp	40.1	C_{18}, 9,10-epoxy, FAME	Bp
13.1	C_6 dioic acid dime	Mic	40.2	9,10,16-diOME C_{16} FAME	Bp
14.3	4-OMe benzaldehyde	Lg P4	40.8	(*m*/*z* 87, 101, 111, 187)	Ps
14.5	methyl indole	Pr	41.0	C_{20} FAME	Lp
15.6	*n*-C_{10} FAME	Lp	41.1	dehydroabietic acid ME	Dt
16.4	4-OMe benzoic acid ME	Lg P6	41.2	18-OMe $C_{18:1}$ FAME	Bp
16.6	3,4,5-tri-OMe benzene	Lg S1	41.5	18-OMe C_{18} FAME	Bp
17.1	dimethyl indole	Pr	41.6	abietic acid ME	Lp/Dt
17.2	3,4-diOMe benzene-4-ethenyl	LgG3	41.8	C_{16}, 9,10,16 tri-OMe-FAME	Bp
17.3	triOMe benzene	Ps	43.0	$C_{18:1}$ dioic acid dime	Bp
17.4	triOMe benzene	Ps	43.5	labd-8-ene-15,18-dioic acid	Lp/Dt
17.5	4-OMe benzeneacetic acid ME	Lg P24	44.5	12-OMe-ferruginol-3-one	Lp/Dt
17.8	(*m*/*z* 88,101)	Ps	44.7	C_{22} FAME	Lp
18.5	(*m*/*z* 88, 101)	Ps	45.3	20-OMe C_{20} FAME	Bp
19.2	C_8 dioic acid DIME	Mic	45.5	9,10,18-tri-OMe C_{18} FAME	Bp
19.6	1*H* indole 5-OMe 2-methyl	Pr	45.8	C_{24}-OMe	Lp
19.7	1-OMe-2-(4-OMe phenyl) ethylene	Lg P7	46.2	C_{23} FAME	Lp
20.8	3,4-diOMe benzaldehyde	Lg G4	46.5	2-OMe C_{22} FAME	Mic
21.0	benzenedicarboxylic acid ME	TMAH	47.0	9,10-diOMe $C_{18:1}$ dioic acid DIME	Bp
21.3	*n*-C_{12} FAME	Lp	47.2	C_{20} dioic acid DIME	Bp
22.2	C_9 dioic acid DIME	Mic	47.6	C_{27} *n*-alkane	Lp
23.0	3,4-diOMe acetophenone	Lg G5	48.3	C_{24} FAME	Lp
23.6	3,4-diOMe benzoic acid ME	Lg G6	48.5	2-OMe C_{23} FAME	Mic
23.9	3,4,5-triOMe benzaldehyde	Lg S4	48.8	22-OMe C_{22} FAME	Bp
24.3	3,4-diOMe benzeneacetic ME	Lg G24	49.3	C_{28} *n*-alkane	Lp
24.6	*cis*-1-(3,4-diOMe phenyl)-2-OMe-ethylene	Lg G7	49.8	C_{26}-OMe	Lp
24.9	*trans*-1-(3,4-diOMe phenyl)-2-OMe-ethylene	Lg G8	50.0	C_{25} FAME	Lp
25.9	4-OMe cinnamic acid ME	P18	50.3	2-OMe C_{24} FAME	Mic
26.1	*cis*-1-(3,4-diOMe phenyl)-1-OMe propene	Lg G10	50.6	C_{22} dioic acid dime	Bp
26.6	3,4,5-triOMe acetophenone	Lg S5	51.0	C_{29} *n*-alkane	Lp
26.8	*n*-C_{14} FAME	Lp	51.7	C_{26} FAME	Lp
26.9	*trans*-1-(3,4-diOMe phenyl)-1-OMe propene	Lg G11	51.9	2-OMe C_{25} FAME	Mic
27.2	triOMe benzoic acid ME	Lg S6	52.2	24-OMe C_{24} FAME	Bp
27.6	*trans*-1-(3,4-diOMe phenyl)-3-OMe propene	Lg G13	52.6	C_{30} *n*-alkane	Lp
28.3	C_{15} iso FAME	Mic	53.2	C_{28}-OMe	Lp
28.5	*cis*-1-(3,4,5-triOMe phenyl)-2-OMe-ethylene	Lg S7	53.5	cholest-5-en-3-OMe	Lp/Tp
28.6	C15 *anteiso* FAME	Mic	53.7	2-OMe C_{26} FAME	Mic
28.9	1-(3,4-diOMe phenyl)-1,2,3-triOMe propane *thr/erit*	Lg G14	53.9	C_{24} dioic acid DIME	Bp
29.1	*trans*-1-(3,4,5-triOMe phenyl)-2-OMe ethylene	Lg S8	54.1	C_{31} *n*-alkane	Lp
29.3	1-(3,4-diOMe phenyl)-1,2,3-triOMe propane *thr/erit*	Lg G15	54.3	campesterol-OMe	Lp/Tp
29.5	*n*-C_{15} FAME	Lp	54.8	C_{28} FAME	Lp
29.6	*trans*-1-(3,4,5-tri OMe phenyl-1-OMe propene	Lg S11	55.4	26-OMe C_{26} FAME	Bp
31.3	1-(3,4-diOMe phenyl)-1,2,3-triOMe propane *thr/erit*	Lg S14	55.5	C_{32} *n*-alkane	Lp
31.7	1-(3,4-diOMe phenyl)-1,2,3-triOMe propane *thr/erit*	Lg S15	55.7	stigmasterol-OMe	Lp/Tp
32.1	*n*-C16 FAME	Lp	56.2	C_{30}-OMe	Lp
32.6	14-OMe C14 FAME	Bp	56.3	C_{29} FAME	Lp
33.3	C_{17} *iso* FAME	Mic	56.6	sitosterol-OMe	Lp/Tp
33.5	C_{17} *anteiso* FAME	Mic	57.0	C_{33} *n*-alkane	Lp
34.2	*n*-C_{17} FAME	Lp	57.3	stigmast-3,5-dien-7-one	Lp/Tp
36.2	$C_{18:1}$ FAME	Lp	57.7	stigmast-4-en-3-one	Lp/Tp
36.6	C_{18} FAME	Lp	58.3	friedelin-OMe	Lp/Tp
37.0	phytol-OMe	Lp	58.6	C_{30} FAME	Lp
37.2	16-OMe C_{16} FAME	Bp	59.1	amyrin-OMe	Lp/Tp
37.3	C_{19} *iso* FAME	Mic	59.6	lupeol-OMe	Lp/Tp
37.5	dehydroabietol-OMe	Dt	60.0	3-OMe-oleanoic acid ME	Lp/Tp
37.9	ferruginol-OMe	Dt	60.5	3-OMe-ursolic acid ME	Lp/Tp

[a] Bp, from plant biopolyesters; Lg, from lignin; Lp, from plant lipids (Dt, diterpenoid; Tp, triterpenoid); Mic, from microbial bioproducts; Pr, from proteins; Ps, from polysaccharides; TMAH, from methylating agent; OMe, methoxy; FAME, fatty acid methyl ester; ME, methyl ester; DIME, dimethyl ester. [b] RT, retention time (min) in total ion chromatogram.

in compost 90 and in the final compost 150, thereby indicating that lignin was hardly oxidized after the first 60 days of compost maturity. These findings, together with the steady total content of guaiacyl and syringyl compounds and the presence of less altered molecules (G14/15, S14/15) in the final compost 150 (**Table 2** and **Figure 3B**), confirm the overall stability of lignin components during composting, as already suggested by NMR spectra.

Alkyl Compounds. Alkyl compounds were the most abundant thermochemolysis products released from compost samples (**Table 2**). The total release yield of compounds, their dimensional ranges, and the dominant homologues are shown in **Table 3**.

As indicated by NMR spectra, the Pyr-TMAH-GC-MS results suggest that hydrophobic alkyl moieties were the main constituents of the less mature compost (**Figure 3A** and **Table 3**).

Table 3. Yields (Micrograms per Gram of Dry Weight)[a] and Composition[b] of Main Thermochemolysis Products Released from Compost Material at Different Compost Maturities

compound	compost 60	compost 90	compost 150
	Lignin Products		
p-hydroxyphenyl	1480	870	650
guaiacyl	3240	2920	2830
Ad/Al_G	3.8 (0.3)	4.1 (0.2)	4.3 (0.3)
Γ_G[c]	2.9 (0.2)	2.8 (0.2)	3.0 (0.1)
syringyl	2950	2710	2730
Ad/Al_S[c]	5.0 (0.2)	4.9 (0.3)	5.1 (0.2)
	Alkyl Products		
fatty acids	36100 $C_{12} \div C_{30}$ ($C_{18:1}$)	15100 $C_{12} \div C_{30}$ ($C_{18:1}$)	13250 $C_{12} \div C_{30}$ ($C_{18:1}$)
>C20 (%)	6.1	14.3	31.2
ω-hydroxy acids	9850 $C_{14} \div C_{26}$ (C_{18})	8150 $C_{14} \div C_{26}$ (C_{16})	7300 $C_{14} \div C_{26}$ (C_{16})
mid-chain hydroxy acids	8350 (C_{16}, C_{18})	6780 (C_{16}, C_{18})	6200 (C_{16}, C_{18})
alkanedioic acids	8150 $C_{18:1} \div C_{24}$ (C_{18})	7300 $C_{18:1} \div C_{24}$ (C_{18})	5900 $C_{18:1} \div C_{24}$ (C_{20})
n-alkanes	3140 $C_{25} \div C_{33}$ (C_{29})	1390 $C_{25} \div C_{33}$ (C_{29})	900 $C_{25} \div C_{33}$ (C_{29})
diterpenoids	2200	2210	2140
triterpenoids	2230	2300	2280

[a] $n = 3$. Overall coefficient of variations: lignin lower than 10%; alkyl lower than 15%. [b] Total range varying from C_i to C_j; compounds in parentheses are the most dominant homologues; number after colon refers to double bond. [c] Structural indices: Ad/Al = G6/G4, S6/S4; Γ_G = G6/(G14 + G15); standard deviation in parentheses.

Compost 60 mostly released methyl esters of linear fatty acid (FAME), with chain length ranging from C_{10} to C_{30}. About 80% of total FAME was made by both saturated and unsaturated hexadecanoic and octadecanoic acids (**Figure 3A**), which are ubiquitous components in living and decayed organisms. The marked predominance of even over odd carbon atoms in FAME indicates the contribution of higher plants to this compost (*34*, *35*). This is supported also by the presence of longer chain FAME, which derive from the breakdown of aliphatic esters and constitute, together with *n*-alkanes and sterols, the external protective wax layer in aerobial plant tissues (*35*). Conversely, a direct input from microbial activity was revealed by the detection of branched chain FAME. Among these, the most abundant compounds were the 12- and 13-methyl tetradecanoic and hexadecanoic acids (iso and anteiso C_{15} and C_{17} FAME in **Table 2**), which are common microbial constituents of natural organic matter (NOM) in terrestrial and marine environments.

Other alkyl molecules in compost 60 were, in order of abundance, the methylated form of midchain hydroxyalkanoic acids, ω-hydroxyalkanoic acids, and alkanedioic acids (**Table 3**). The mono-, di-, and trihydroxy acids were represented only by the C_{16} and C_{18} homologues, with 9,16- and 10,16-dihydroxyhexadecanoic isomers being the most abundant products, followed by 9,10,18-trihydroxyoctadecanoic acid and other C_{16} and C_{18} components in minor amounts (**Figure 3A**). The hexadecanoic and monounsaturated octadecanoic acids were the main ω-hydroxyalkanoic acids, the minor components ($C_{14}-C_{26}$) of which showed a wide range of even carbon numbered units. The alkanedioic acids were characterized by two well-distinct short-chain (C_6-C_{10}) and long-chain ($C_{18}-C_{24}$) groups, the latter also including the monounsaturated $C_{18:1}$ acid as the principal product (**Table 2**). Among the heaviest components, another C_{18} homologue was tentatively identified, on the basis of mass spectra, as the 9,10-dihydroxyoctadecandioc acid.

A significant amount of straight-chain alkanes was released from compost 60. Their exclusive presence as long-chain hydrocarbons (**Table 2**), the distinct predominance of odd versus even carbon numbers (**Figure 3A**), and the large amount of nonacosane, hentriacontane, and tritriacontane all suggested a prevalent origin of these alkanes from wax layers of higher plants (*36*).

Tricyclic diterpenes and tetra- and pentacyclic triterpenes were distinctly identified, although in low amount, among the thermochemolysis products from compost 60 (**Tables 2** and **3**). The abietic, pimaric, and isopimaric acids were the main original precursors found among the diterpenoid molecules, followed by their diagenetic products, such as dehydroabietane and dehydroabietic acid and labdane acid derivatives. The diterpenic acids, especially those with abietane and pimarane skeletons, are the most representative component of natural diterpenoids, currently found in resins of various higher plants such as Coniferae and Leguminosae families (*37*). The tetracyclic triterpenes found in compost 60 were represented by methyl ethers and esters of methyl/ethyl cholesten-3-ol derivatives, whereas pentacyclic triterpenes were the ursane, lupeane, and oleanane structures. Both sterol and triterpenol compounds are among the most abundant lipid components of plant tissues (*38*, *39*). It has been already pointed out that sterol and triterpenol of plant residues undergo a rapid decline once exposed to microbial activity (*35*, *38*). Therefore, their relatively low amount in compost 60 may be explained by the biotic and abiotic degradation occurring at the initial active phase of composting. Both diterpenoid and triterpenoid compounds are useful indicators of coniferous and angiosperm plants in terrestrial and marine environments (*40*), because the structural characteristics of their original precursors are maintained despite the various degradation processes undergone by the plant species (*41*). Conversely, biomarkers of microbial activity in altered natural organic matter are the 2-hydroxyalkanoic acids (*26*), which were also found in low amount in compost samples (**Table 2**).

The alkyl composition found here by thermochemolysis agrees with the results shown by Spaccini and Piccolo (*10*), who characterized the molecular composition of the same compost materials by applying a sequential chemical fractionation (*10*). The linear fatty acids, alkanes, sterol, and diterpenes released by thermochemolysis closely resembled the components extracted from compost by an organic solvent (*10*), thereby indicating that the thermal treatment effectively favored the transfer in the gas phase of the alkyl molecules, which were only physically entrapped in the compost matrix. Both hydroxyalkanoic and alkanedioic acids were released from compost by progressively stronger hydrolytic treatments and, thus, assumed to be chemically bound to the compost matrix (*10*). Also in the case of the thermochemolysis applied here, whereas the short-chain alkanedioic acids may result from biotic and abiotic

oxidation of longer chain monounsaturated acids (*25*), the released longer chain molecules represent the building block of plant bio-polyesters (*42*, *43*) and, thus, compost components strongly bound in an extensive network of intra- and intermolecular ester bonds. Therefore, the large range and high yield of methyl ether/ester derivatives of alkyl monomers released by thermochemolysis of compost (**Tables 2** and **3**) indicate the Pyr-TMAH-GC-MS technique is a rapid and effective alternative to the chemical stepwise fractionation for the molecular characterization of complex compost substrates.

The amount of components released by Pyr-TMAH-GC-MS decreased progressively with increasing maturity of compost samples. A much larger loss of alkyl compounds was noted by passing from compost 60 to 90 than from compost 90 to the final mature compost 150 (**Table 3**). However, the thermochemolysis products released from compost 150 were still dominated by alkyl compounds but with a different relative distribution (**Figure 3**).

Linear fatty acids and hydrocarbons decreased by 65 and 72% after 150 days of compost stabilization, respectively. The hexadecanoic and octadecanoic acids were most significantly affected by the composting process, whereas greater stability and, thus, detectability were shown by longer chain fatty acids, which were even increased by 25% relative to the total amount of FAME (**Table 3**). A small variation with composting was revealed by the overall *n*-alkane distribution, with a slightly higher preservation of the heaviest components.

A larger persistence with compost maturity was noted for the various products deriving from aliphatic bio-polyesters, as is revealed by the relative increase of signal intensity in the compost 150 pyrogram (**Figure 3B**). Total yields showed their partial decrease passing from compost 60 to 90, although about 70% of components found in compost 60 were still released from compost 150 (**Table 3**). For ω-hydroxy- and alkanedioic acids, the degradation was more selective for the monounsaturated C_{18} compounds, owing to the biochemical lability of the internal double bond, whereas lower losses during composting were shown by the long-chain saturated homologues. Despite the decrease of some minor components, an unexpected high amount of midchain hydroxyalkanoic acids was found in compost 150. This is in contrast with the reported intrinsic biolability of the midchain oxygen functionality of these compounds (*44*, *45*).

The largest alkyl loss, which occurred between 60 and 90 days of composting (**Table 3**), is in line with the large decrease of alkyl carbons that was observed in NMR spectra of compost 90 (**Table 1** and **Figure 1B**). This may be due to the decomposition of structurally unbound, and thus easy bioavailable, fatty acids and *n*-alkanes. The greater access of linear alkyl acids and hydrocarbons to microbial decomposition agrees with the fact that these components are preferentially extracted in organic solvents as unbound components (*10*, *35*, *38*).

The relative persistence of different alkyl bio-polyesters, at increasing compost maturity, is in agreement with previous findings on NOM. Both hydroxyalkanoic acids and alkanedioic acids are currently found among the main thermochemolysis products of persistent soil organic fractions such as humic acids and humin (*25*, *26*). Moreover, the selective preservation of these hydrophobic molecules was recognized among the main factors leading to the accumulation of recalcitrant organic compounds in soil (*18*, *46*). Our findings confirm the key role of hydrophobic compounds in the stabilization of complex natural organic matter, such as compost, during biological transformation.

No significant changes with compost maturity were found in amount and composition of tricyclic diterpenes and tetra- and pentacyclic triterpenes. Sterols and triterpenols were in fact among the main Pyr-TMAH-GC-MS products of compost 150 (**Table 3**). This confirms that triterpenoid and diterpenoid compounds may survive relatively unaltered the biological decay of dead tissues and represent useful biomarkers to trace molecular inputs of higher plants into NOM (*40*).

Our results indicate that the offline Pyr-TMAH-GC-MS technique is a rapid and effective method to obtain direct qualitative and quantitative evaluation of complex organic materials. This technique can be efficiently applied for the direct molecular characterization of bulk compost substrates, thereby replacing, with equal molecular resolution, a more lengthy, although detailed, stepwise chemical fractionation procedure. Plant biopolymers such as lignin, waxes, and aliphatic polyesters were recognized as the main sources of composted organic material. Moreover, the offline Pyr-TMAH-GC-MS technique provided a detailed evaluation of the compost molecular modifications during the maturity process and of the various lignin and alkyl biomarkers, which are useful to trace both the origin of compost substrates and the fate of compost in the environment.

LITERATURE CITED

(1) Spaccini, R.; Conte, P.; Piccolo, A.; Haberhauer, G.; Gerzabek, M. H. Increased soil organic carbon sequestration through hydrophobic protection by humic substances. *Soil Biol. Biochem.* **2002**, *34*, 1839−1851.

(2) Piccolo, A.; Spaccini, R.; Nieder, R.; Richter, J. Sequestration of a biologically labile organic carbon in soils by humified organic matter. *Climatic Change* **2004**, *67*, 329−343.

(3) Conte, P.; Agretto, A.; Spaccini, R.; Piccolo, A. Soil remediation: humic acids as natural surfactants in the washings of highly contaminated soils. *Environ. Pollut.* **2005**, *135*, 515−522.

(4) Quagliotto, P.; Montoneri, E.; Tambone, F.; Adani, F.; Gobetto, R.; Viscardi, G. Chemicals from wastes: compost-derived humic acid-like matter as surfactant. *Environ. Sci. Technol.* **2006**, *40*, 1686−1692.

(5) Chefetz, B.; Hatcher, P. G.; Hadar, Y.; Chen, Y. Characterization of dissolved organic matter extracted from composted municipal solid waste. *Soil Sci. Soc. Am. J.* **1998**, *62*, 326−332.

(6) Veeken, A.; Nierop, K.; de Wilde, V.; Hamelers, B. Characterisation of NaOH extracted humic acids during composting of a biowaste. *Bioresour. Technol.* **2000**, *72*, 33−41.

(7) Castaldi, P.; Alberti, G.; Morella, R.; Melis, P. Study of the organic matter evolution during municipal solid waste composting aimed at identifying suitable parameters for the evaluation of compost maturity. *Waste Manag.* **2005**, *25*, 209−213.

(8) Baddia, G. A.; Alburquerque, J. A.; Gonzálvez, J.; Cegarra, J.; Hafidi, M. Chemical and spectroscopic analyses of organic matter transformations during composting of olive mill wastes. *Int. Biodeter. Biodeg.* **2004**, *54*, 39−44.

(9) González-Vila, F. J.; Almendros, G.; Madrid, F. Molecular alteration of organic fractions from urban waste in the course of composting and their further transformation in amended soil. *Sci. Total Environ.* **1999**, *236*, 215−229.

(10) Spaccini, R.; Piccolo A. Molecular characterization of compost at increasing stages of maturity. 1. Chemical fractionation and infrared spectroscopy. *J. Agric. Food Chem.* **2007**, *55*, 2293−2302.

(11) Del Rio, J. C.; McKinney, D. E.; Knicker, H.; Nanny, M. A.; Minard, R. D.; Hatcher, P. G. Structural characterization of bio-

and geo-macromolecules by off-line thermochemolysis with tetramethylammonium hydroxide. *J. Chromatogr. A* **1998**, *823*, 443−448.

(12) Kogel-Knabner, I. The macromolecular organic composition of plant and microbial residues as inputs to soil organic matter. *Soil Biol. Biochem.* **2002**, *34*, 139−162.

(13) Clifford, D. J.; Carson, D. M.; McKinney, D. E.; Bortiatynsky, J. M.; Hatcher, P. G. A new rapid technique for the characterization of lignin in vascular plant: thermochemolysis with tetramethylammonium hydroxide (TMAH). *Org. Geochem.* **1995**, *23*, 169−175.

(14) Nierop, K. G. J.; Pulleman, M. M.; Marinissen, J. C. Y. Management induced organic matter differentiation in grassland and arable soils: a study using pyrolysis techniques. *Soil Biol. Biochem.* **2001**, *33*, 755−764.

(15) Wang, L.; Ando, S.; Ishida, Y.; Ohtani, H.; Tsuge, S.; Nakayama, T. Quantitative and discriminative analysis of carnauba waxes by reactive pyrolysis-GC in the presence of organic alkalin using a vertical microfurnace pyrolyzer *J. Anal. Appl. Pyrol.* **2001**, *58−59*, 525−537.

(16) de Leeuw, J. W.; Baas, W. J. The behaviour of esters in the presence of tetramethylammonium salts at elevated temperatures; flash pyrolysis or flash chemolysis? *J. Anal. Appl. Pyrol.* **1993**, *26*, 175−184.

(17) Filley, T. R.; Minard, R. D.; Hatcher, P. G. Tetramethylammonium hydroxide (TMAH) thermochemolysis: proposed mechanism based upon the application of ^{13}C-labeled TMAH to a synthetic model lignin dimer. *Org. Geochem.* **1999**, *30*, 607−621.

(18) Grasset, L.; Amblès, A. Structural study of soil humic acids and humin using a new preparative thermochemolysis technique. *J. Anal. Appl. Pyrol.* **1998**, *47*, 1−12.

(19) Spaccini, R.; Mbagwu, J. S. C.; Igwe, C. A.; Conte, P.; Piccolo, A. Carbohydrates and aggregation in lowland soils of Nigeria as influenced by organic inputs. *Soil Till. Res.* **2004**, *75*, 161−172.

(20) Hatcher, P. G. Chemical structure studies of natural lignin by dipolar dephasing solid-state ^{13}C nuclear magnetic resonance *Org. Geochem.* **1987**, *11*, 31−39.

(21) Vane, C. H.; Martin, S. C.; Snape, C. E.; Abbott, G. D. Degradation of lignin in wheat straw during growth of the oyster mushroom (*Pleurotus ostreatus*) using off-line thermochemolysis with tetramethylammonium hydroxyde and solid state ^{13}C NMR *J. Agric. Food Chem.* **2001**, *49*, 2709−2716.

(22) Atalla, R. H.; VanderHart, D. L. The role of solid state ^{13}C NMR spectroscopy in studies of the nature of native celluloses. *Solid State Nucl. Magn. Reson.* **1999**, *15*, 1−19.

(23) Hatcher, P. G.; Nanny, M. A.; Minard, R. D.; Dible, S. D.; Carson, D. M. Comparison of two thermochemolytic methods for the analysis of lignin in decomposing gymnosperm wood: the CuO oxydation method and the method of thermochemolysis with tetramethylammonium hydroxide (TMAH). *Org. Geochem.* **1995**, *23*, 881−888.

(24) Johnson, C. E.; Smernik, R. J.; Siccama, T. G.; Kiemle, D. K.; Xu, Z.; Vogt, D. J. Using ^{13}C nuclear magnetic resonance spectroscopy for the study of northern hardwood tissues. *Can. J. For. Res.* **2005**, *35*, 1821−1831.

(25) Grasset, L.; Guignard, C.; Amblès, A. Free and esterified aliphatic carboxylic acids in humin and humic acids from a peat sample as revealed by pyrolysis with tetramethylammonium hydroxide or tetraethylammonium acetate. *Org. Geochem.* **2002**, *33*, 181−188.

(26) Guignard, C.; Lemée, L.; Amblès, A. Lipid constituents of peat humic acids and humin. Distinction from directly extractable bitumen components using TMAH and TEAAc thermochemolysis. *Org. Geochem.* **2005**, *36*, 287−297.

(27) Chefetz, B.; Chen, Y.; Clapp, C. E.; Hatcher, P. G. Characterization of organic matter in soils by thermochemolysis using tetramethylammonium hydroxide (TMAH). *Soil Sci. Soc. Am. J.* **2000**, *64*, 583−589.

(28) Schwarzinger, C.; Tanczos, I.; Schmidt, H. Levoglucosan, cellobiose and their acetates as model compounds for the thermally assisted hydrolysis and methylation of cellulose and cellulose acetate. *J. Anal. Appl. Pyrol.* **2002**, *62*, 179−196.

(29) Martin, F.; del Rio, J. C.; Gonzàlez-Vila, F.-J.; Verdejo, T. Thermally assisted hydrolysis and alkylation of lignins in the presence of tetra-methylammonium hydroxides. *J. Anal. Appl. Pyrol.* **1995**, *35*, 1−13.

(30) Vane, C. H.; Abbott, G. D.; Head, I. M. The effect of fungal decay (*Agaricus bisporus*) on wheat straw lignin using pyrolysis-GC-MS in the presence of tetramethylammonium hydroxide (TMAH). *J. Anal. Appl. Pyrol.* **2001**, *60*, 69−78.

(31) Goñi, M. A.; Hedges, J. I. Lignin dimers: structures, distribution, and potential geochemical applications. *Geochim. Cosmochim. Acta* **1992**, *49*, 2097−2107.

(32) Nierop, K. G. J. Temporal and vertical organic matter differentiation along a vegetation succession as revealed by pyrolysis and thermally assisted hydrolysis and methylation. *J. Anal. Appl. Pyrol.* **2001**, *61*, 111−132.

(33) Vane, C. H.; Drage, T. C.; Snape, C. L. Biodegradation of oak (*Quercus alba*) wood during growth of the shiitake mushroom (*Lentinula edodes*): a molecular approach. *J. Agric. Food Chem.* **2003**, *51*, 947−956.

(34) Amblès, A.; Jambu, P.; Parlanti, E.; Joffre, J.; Riffe, C. Incorporation of natural monoacids from plant residues into a hydromorphic forest podzol. *Eur. J. Soil Sci.* **1994**, *45*, 175−182.

(35) Naafs, D. F. W.; van Bergen, P. F.; de Jong, M. A.; Oonincx, A.; de Leeuw, J. W. Total lipid extracts from characteristic soil horizons in a podzol profile. *Eur. J. Soil Sci.* **2004**, *55*, 657−669.

(36) Lichtfouse, E. Plant wax *n*-alkanes trapped in soil humin by noncovalent bonds. *Naturwissenschaften* **1998**, *85*, 449−452.

(37) Pastorova, I.; van der Berg, K. J.; Boon, J. J.; Verhoeven, J. W. Analysis of oxidised diterpenoid acids using thermally assisted methylation with TMAH. *J. Anal. Appl. Pyrol.* **1997**, *43*, 51−57.

(38) Bull, I. D.; Nott, C. J.; van Bergen, P. F.; Poulton, P. R.; Evershed, R. P. Organic geochemical studies of soils from the Rothamsted classical experiments—V. The fate of lipids in different long-term experiments. *Org. Geochem.* **2000**, *31*, 389−408.

(39) Nierop, K. G. J.; Naafs, D. F. W.; Verstraten, J. M. Occurrence and distribution of ester-bound lipids in Dutch coastal dune soils along a pH gradient. *Org. Geochem.* **2003**, *34*, 719−729.

(40) Otto, A.; Simoneit, B. R. T. Chemosystematics and diagenesis of terpenoids in fossil conifer species and sediment from the Eocene Zeitz formation, Saxony, Germany. *Geochim. Cosmochim. Acta* **2001**, *65*, 3505−3527.

(41) van Bergen, P. F.; Bull, I. D.; Poulton, P. R.; Evershed, R. P. Organic geochemical studies of soils from the Rothamsted Classical Experiments—I. Total lipid extracts, solvent insoluble residues and humic acids from Broadbalk Wilderness. *Org. Geochem.* **1997**, *26*, 117−135.

(42) McKinney, D. E.; Bortiatynsky, J. M.; Carson, D. M.; Clifford, D. J.; de Leeuw, J. W.; Hatcher, P. G. Tetramethylammonium hydroxyde (TMAH) thermochemolysis of the aliphatic biopolymer cutan: insights into the chemical structure. *Org. Geochem.* **1996**, *24*, 641−650.

(43) Santos Bento, M. F.; Pereira, H.; Cunha, M. Á.; Moutinho, A. M. C.; van der Berg, K. J.; Boon, J. J. A study of variability of suberin composition in cork from *Quercus suber* L. using thermally assisted transmethylation GC-MS. *J. Anal. Appl. Pyrol.* **2001**, *57*, 45−55.

(44) Goñi, M. A.; Hedges, J. I. The diagenetic behaviour of cutin acids in buried conifer needles and sediments from a coastal

marine environment. *Geochim. Cosmochim. Acta* **1990**, *54*, 3083−3093.

(45) Opsahl, S.; Benner, R. Early diagenesis of vascular plant tissues: lignin and cutin decomposition and biogeochemical implications. *Geochim. Cosmochim. Acta* **1995**, *59*, 4889−4904.

(46) Almendros, G.; Sanz, J. Structural study on the soil humin fraction—boron trifluoride−methanol transesterification of soil humin preparation. *Soil Biol. Biochem.* **1991**, *23*, 1147−1154.

Received for review September 4, 2006. Revised manuscript received January 4, 2007. Accepted January 5, 2007. This work was partially supported by Grant MIUR−COFIN 2005 "Structure−activity relationships of natural organic matter in plant-soil systems".

JF0625407